



## Gas enclosure in polar firn follows universal law

Christoph Florian Schaller<sup>1</sup>, Johannes Freitag<sup>1</sup>, and Olaf Eisen<sup>1,2</sup>

<sup>1</sup>Alfred Wegener Institute, Helmholtz Centre for Polar and Marine Research, D-27568 Bremerhaven, Germany

<sup>2</sup>Department of Geosciences, University of Bremen, D-28359 Bremen, Germany

*Correspondence to:* Christoph Florian Schaller ([christoph.schaller@awi.de](mailto:christoph.schaller@awi.de))

**Abstract.** In order to interpret the paleoclimatic record stored in the air enclosed in polar ice cores, it is crucial to understand the fundamental lock-in process. Within the porous firn, bubbles are sealed continuously until the respective horizontal layer reaches a critical porosity. Present-day firn models use a postulated temperature dependence of this value as the only parameter to adjust to the surrounding conditions of individual sites. However, no direct measurements of the firn microstructure could confirm these assumptions. Here we show that the critical porosity is a universal constant by providing a statistically solid data set of  $\mu\text{m}$ -resolution 3D X-ray computer tomographic measurements for ice cores representing different extremes of the temperature and accumulation ranges. We demonstrate why indirect measurements yield misleading data and substantiate our observations by applying percolation theory as a theoretical framework for bubble trapping. Incorporation of our results does significantly influence the dating of trace gas records, changing gas age–ice age differences by up to more than 1000 years. This will help resolve inconsistencies, such as differences between East Antarctic  $\delta^{15}\text{N}$  records (as a proxy for firn height) and model results. We expect our findings to be the basis for improved firn air and densification models, leading to lower dating uncertainties. The reduced coupling of proxies and surrounding conditions may allow for more sophisticated reinterpretations of trace gas records in terms of paleoclimatic changes and will foster the development of new proxies, such as the air content as a marker of local insolation.

### 15 1 Introduction

Air trapped in polar ice cores provides a unique opportunity for paleoclimatic studies (Legrand and Mayewski, 1997). In particular, it allows reconstruction of the past chemical and isotopic composition of the atmosphere for up to 800,000 years (Jouzel et al., 2007; Loulergue et al., 2008). However, it is not a direct record as bubbles are only isolated from the atmosphere at a certain depth, the firn-ice transition (50–120 m depending on the local conditions). As a result, the enclosed air is always younger than the surrounding ice. Accurate estimation of this gas age–ice age difference ( $\Delta\text{age}$ ), up to 7000 years during glacial periods (Bender et al., 2006), is essential for the interpretation of ice-core records as otherwise phase relationships between ice and gas records cannot be determined safely.

Thus, it is crucial to understand the fundamental processes in the porous firn (Schwander and Stauffer, 1984) – diffusion of air through the open pore space (Trudinger et al., 1997; Fabre et al., 2000) and the entrapment of air by bubble closure due to firn densification, which is the main focus of this study. In a depth range referred to as the lock-in zone, individual horizontal layers close off at a critical porosity (Schwander et al., 1993). It is the only parameter in empirical relations of closed and total



porosity (Schwander, 1989; Goujon et al., 2003) that are commonly used in present-day firn models (Severinghaus and Battle, 2006; Mitchell et al., 2015). A temperature dependence of this value has been postulated (Raynaud and Lebel, 1979) and parametrized using air-content measurements (Martinerie et al., 1992). Nonetheless, the underlying microstructural processes are not understood and there is no confirmation of these assumptions by direct measurements.

5 The  $\delta^{15}\text{N}$  of  $\text{N}_2$  has been established as a proxy for firn height and thus  $\Delta_{\text{age}}$  (Sowers et al., 1992). This relation has successfully been tested for high-accumulation sites, e.g. Greenland (Severinghaus et al., 1998), showing good agreement with other dating methods. On the contrary, there is a mismatch of up to 2000 years with model results for the East Antarctic plateau (Bender et al., 2006; Parrenin et al., 2012). These modeled chronologies are based on the current knowledge of bubble trapping in polar firn and particularly sensitive to the critical porosity via the assumed temperature dependence. Recently the  
10 inclusion of impurity effects has reduced the mismatch for East Antarctic sites, however it deteriorates the agreement between modelled and measured  $\delta^{15}\text{N}$  for high-accumulation sites (Breant et al., 2017).

In this paper, we present the first statistically solid data set of direct firn microstructure measurements throughout the lock-in zone. We start off by using it to scrutinize the current knowledge of gas enclosure in polar firn and show why previous indirect measurements yielded misleading results. Then, we apply percolation theory (Enting, 1993) as a theoretical framework for our  
15 conclusions and demonstrate their agreement with other methods. Finally, we discuss changes in the dating and interpretation of trace-gas records that incorporation of our results in current firn models will imply. The reduced coupling of proxies and surrounding conditions may allow for more sophisticated reinterpretations in terms of paleoclimatic changes and will foster the development of new proxies, such as the air content as a marker of local insolation (Raynaud et al., 2007; Eicher et al., 2016).

## 2 Materials and Methods

20 Firn microstructure throughout the lock-in zone has been deduced for ice cores from three locations (cf. Table 1) using a specifically designed X-ray microfocuss computer tomograph in a cold lab (Freitag et al., 2013). For each one meter core segment, we scanned a minimum number of five sections of approximately 4 cm height and the full core diameter (8–10 cm) with a focus on homogenous layers. One measurement consists of 3,000 radioscopic images, which are used to tomographically reconstruct the 3D microstructure at a resolution of approximately 25  $\mu\text{m}$  (e.g. Fig. 1b). Consecutively, these reconstructions  
25 are segmented into ice and air using a two-step procedure consisting of a two-level Otsu's method followed by simple region growing for the ambiguous voxels. We adapted an existing algorithm (Nguyen et al., 2011) to determine the coordination number during the segmentation process. To eliminate the effect of cut bubbles at the surface of the sample (Martinerie et al., 1990), each data point corresponds to a layer of approximately 1 cm height and 6 cm diameter. Having the microstructure of the surrounding material in all directions at hand allows us to safely determine whether a pore is open or closed. For all  
30 measurements, the remaining cut bubbles were less than 0.1% of the pore volume. For ten repeat measurements of the same sample, both standard and maximum deviation of the total porosity are less than 1%. Furthermore, the total porosities agree with those from bulk measurements and 2D radioscopy with a maximum deviation of 3%.



A well-known framework to model porous media is bond percolation theory (Broadbent and Hammersley, 1957). It enables us to predict the point at which a material becomes impermeable. The Kelvin structure (packed tetrakaidecahedra, see Fig. 1a) is space-filling with one of the lowest surface-area-to-volume ratios. It is well-studied and has for example been applied as a model for foam (Koehler et al., 1999). We use it to represent sintered ice grains. When packed, the grains align along a body-centered cubic lattice. Therefore the air network corresponds to its dual lattice which has a coordination number (average number of neighbors) of four when fully occupied. Its percolation threshold, the percentage of channels occupied by air at close-off, is known to be 0.4031 (van der Marck, 1997). Thus the predicted coordination number at close-off is  $4 \cdot 0.4031 = 1.6124$ . Notably, the influence of the chosen lattice is rather small (Wierman and Naor, 2003).

### 3 Results

Lock-in of bubbles occurs at the same critical porosity  $\Phi_{\text{crit}}$  of about 0.1 for all cores (Fig. 2a). However, gas enclosure takes place in a significantly smaller porosity range for the East Antarctic cores compared to the coastal Greenland site leading to a much steeper slope of the closed porosity. To fit our data, we derived a new local relation (Eq. (1)) of closed and total porosity, where  $b, \lambda_1, \lambda_2 \in \mathbb{R}_{\geq 0}$  and  $b \leq 1$ . The parameters of least squares fitting are given in Table 2.

$$\Phi_{\text{cl}} = \begin{cases} \Phi & \text{for } \Phi \leq \Phi_{\text{crit}} \\ \Phi_{\text{crit}} (b e^{-\lambda_1(\Phi - \Phi_{\text{crit}})} + (1 - b) e^{-\lambda_2(\Phi - \Phi_{\text{crit}})}) & \text{else} \end{cases} \quad (1)$$

In order to estimate the effect of bubbles cut during ice-core processing we mimic sample properties comparable to the ones used for Summit, Greenland (Schwander et al., 1993) in our microstructure analysis. Thereby we ignore our knowledge of the surrounding material and count all cut bubbles as part of the open pore space. This significantly changes the shape of the curve and yields results similar to previous studies (Fig. 2b).

For the coordination number (Fig. 1c) we observe a linear increase with total porosity for all three sites. At the critical porosity of about 0.1 we obtain very similar values of  $1.65 \pm 0.17$  for B53,  $1.7 \pm 0.18$  for B49 and  $1.64 \pm 0.24$  for RECAP\_S2 from linear regression.

### 4 Discussion

Even though the surrounding conditions differ significantly, we obtain the same critical porosity of about 0.1 for all cores (Fig. 2a, Table 2). In previous literature, ice densities at air isolation level were obtained from air-content measurements on deep ice samples (Martinerie et al., 1992). To allow for a better comparison with our results, we calculated the corresponding critical porosities (Fig. 3). We do not observe the commonly assumed temperature dependence of  $\Phi_{\text{crit}}$ . In contrast, we find strong evidence for a constant critical porosity.

Previous studies relied on measuring the gas left in a sample by melting it in a vacuum chamber. However, this does not only extract the air from the open pore space, but also cut closed pores. Breaking of closed, but still fragile pores might even



enhance this effect (Schwander and Stauffer, 1984). Nonetheless it has been neglected or only accounted for by multiplying with correction factors of less than 10% to date (Martinerie et al., 1990; Mitchell et al., 2015). Our estimation (Fig. 2b) proves a serious underestimation of the cut bubble effect and, in particular, confirms the existence of a critical porosity in contrast to recent assumptions of single-layer close-off occurring within a certain porosity range (Mitchell et al., 2015).

5 Due to the lack of undisturbed measurements, notions such as close-off of layers occurring at a critical closed (Goujon et al., 2003) or open (Gregory et al., 2014) porosity have become widely accepted. These approaches have to be considered attempts to obtain agreement with corrupted measurements. Interestingly, the critical closed porosity value of 37% identified by Barnola using porosity measurements of several ice cores from Greenland and Antarctica (Goujon et al., 2003) corresponds to a total porosity of 0.1 for the two corrupted data sets displayed in Fig. 2b (Summit and B53). Nonetheless, we want to strongly  
10 encourage the future avoidance of such concepts – at "close-off" a layer should have a closed porosity of 100% by definition.

Remarkably, for the correct critical porosity, the Schwander parametrization (Schwander, 1989) seems to approximately represent a site-independent average relation of closed and total porosity. However, due to the lack of other parameters, it cannot resemble the true behavior of the firm. Therefore we decided to derive a more complex exponential-decay relation (Eq. (1)) to fit our results.

15 For all three cores, the observed coordination numbers at close-off (Fig. 1c) are in agreement with the value predicted by percolation theory. We conclude that polar firm evolves towards the same "optimal" microstructure, driven by a universal percolation process (Enting, 1993). However, the initial conditions differ as the firm is strongly influenced by the surrounding local conditions such as accumulation rate (affecting residence times in certain depth intervals) and temperature (as one of the main drivers for snow and firm metamorphism (Schneebeli and Sokratov, 2004)).

20 The results of two firm air pumpings conducted at the RECAP drill site (T. Sowers, personal communication, 2017) and at Kohnen station, close to B49 (Weiler, 2008) in combination with high-resolution X-ray porosity measurements (Freitag et al., 2013), further confirm our findings. For both sites, the sharp decline in CO<sub>2</sub>, CH<sub>4</sub> and N<sub>2</sub>O concentrations (commonly interpreted as the onset of the lock-in zone) coincides with the occurrence of the first significant (i.e. at least 1 cm thick) layer with a porosity below 0.1. On the other hand, no more air can be pumped when there are no further layers with a total porosity  
25 larger than 0.1. Thus the limits of the lock-in zone are solely determined by the existence of significant layers above and below the critical porosity, and thereby the (cm-scale) porosity variability.

Even though a single layer closes off at the same critical porosity, sealed layers may have variable air contents. Above the close-off depth, we determine average coefficients of variation for the total porosity of 1.3% for B53, 1.8% for B49 and 2.5% for RECAP\_S2. Higher porosity variability will lead to a larger amount of shallowly trapped bubbles, thereby increasing the  
30 air content  $V$  (Stauffer et al., 1985). In our case, shallow trapping is characterized by the different slopes of the lock-in curves given in Fig. 2a, leading to increased air contents of about 2% for B49 and 8% for RECAP\_S2 in comparison with B53. In addition, the lock-in zone extends over a depth range of approximately 7 m for B53, 9 m for B49 and 15 m for RECAP\_S2. Larger lock-in zones are expected to cause enhanced sealing effects (i.e. permeable layers being sealed by impermeable ones above). This further increases the air content (Stauffer et al., 1985). The effect is hard to quantify as our measurements do not  
35 yield information about the spatial extent of horizontal layers. Nonetheless it may explain the 8% and 27% larger air contents



for B49 and RECAP\_S2 (compared to B53) respectively, that  $V$  measurements for deep ice cores would predict (Martinerie et al., 1992).

We conclude that  $V$  measurements may yield multiple-layer averages of pore volumes at close-off. They should only be interpreted with great caution in regards to the sealing of single layers. The post-coring loss of enclosed air is an error source we can neither quantify nor rule out. For the Camp Century core about 10% lower air contents were observed after 35 years of storage (Vinther et al., 2009), although a systematic error due to the different measurement setups is possible.

## 5 Implications

For the EDC core (East Antarctica), 86% of the variance in  $V$  cannot be explained by air pressure or temperature changes. An anti-correlation with local insolation was found and suggested as a new proxy (Raynaud et al., 2007). The same insolation signature was found for the  $V$  record of the NGRIP core (Greenland), but the underlying physical mechanisms are not yet resolved (Eicher et al., 2016). Based on our results, we rule out the idea of other properties influencing the porosity at close-off for single layers as we do not even observe a temperature dependence. Instead, we suggest increased sealing effects and shallow trapping due to larger porosity variability of the layered snowpack as an explanation. Reasons for the enhanced layering may be changes in the atmospheric conditions, accumulation rate or impurity content, similar to the observed increase in layering during glacials (Augustin et al., 2004).

Up-to-date firn models seem to have difficulties to estimate past lock-in depths compared to  $\delta^{15}\text{N}$  measurements (Sowers et al., 1992) and to synchronize age dating of individual ice cores (Parrenin et al., 2012). We suggest that incorporation of our results will help to overcome these problems, as current approaches are based on temperature-dependent lock-in (Martinerie et al., 1992) and the Barnola model (Goujon et al., 2003). Exemplarily, we calculate the gas age–ice age difference for the Vostok ice core from the temperature (Jouzel et al., 1987) and accumulation rate (Parrenin, 2004) records using the Herron-Langway model (Herron and Langway, 1980). On average, this reduces the gas age–ice age difference by well over 10%. For the last glacial more than 1000 years of the 2000 year mismatch with  $\delta^{15}\text{N}$  data (Bender et al., 2006) can be explained this way. We suggest a combination with the effect of impurities on firn densification (Freitag et al., 2013; Breant et al., 2017) as a promising approach to resolve the remaining mismatch. Other effects that are currently not well represented, such as stronger layering during the glacials (Bendel et al., 2013), may further influence these values. We see this study as a catalyst for improved firn air and densification models, that will reduce dating uncertainties and allow for more sophisticated reinterpretations of the available trace gas records, in particular due to the reduced coupling to temperature.

*Code and data availability.* The data shown in the plots will be uploaded to the open-access library PANGAEA<sup>®</sup>. If you are interested in using our implementation of the described algorithms or want to work with the raw data, please contact the main author.



*Author contributions.* JF was responsible for the development of the AWI ICE-CT and pointed out the opportunity for this study to CS. 3D measurements were carried out by JF for RECAP\_S2 and CS for B49 and B53. The segmentation of the 3D data sets and the evaluation of microstructural parameters was performed by CS, who researched and programmed the necessary algorithms. The results and their implications were discussed and related to the literature by all co-authors. CS prepared the initial manuscript, which was reviewed and improved by all co-authors.

5

*Competing interests.* The authors declare no conflict of interest.

*Acknowledgements.* The authors want to acknowledge Sepp Kipfstuhl and Bo Vinther as the responsables for the drilling of B49/B53 and RECAP\_S2 respectively and Todd Sowers for providing an insight into the RECAP firn-air data. The main author wants to thank the German National Merit Foundation (Studienstiftung des deutschen Volkes e.V.) for funding his PhD project.



## References

- Augustin, L., Barbante, C., Barnes, P. R., Barnola, J.-M., Bigler, M., Castellano, E., Cattani, O., Chappellaz, J., Dahl-Jensen, D., Delmonte, B., and others: Eight glacial cycles from an Antarctic ice core, *Nature*, 429, 623–628, <http://www.nature.com/nature/journal/v429/n6992/abs/nature02599.html>, 2004.
- 5 Bendel, V., Ueltzhöffer, K. J., Freitag, J., Kipfstuhl, S., Kuhs, W. F., Garbe, C. S., and Faria, S. H.: High-resolution variations in size, number and arrangement of air bubbles in the EPICA DML (Antarctica) ice core, *J. Glaciol.*, 59, 972–980, <https://doi.org/10.3189/2013JoG12J245>, 2013.
- Bender, M. L., Floch, G., Chappellaz, J., Suwa, M., Barnola, J.-M., Blunier, T., Dreyfus, G., Jouzel, J., and Parrenin, F.: Gas age-ice age differences and the chronology of the Vostok ice core, 0–100 ka, *J. Geophys. Res.*, 111, <https://doi.org/10.1029/2005JD006488>, 2006.
- 10 Breant, C., Martinerie, P., Orsi, A., Arnaud, L., and Landais, A.: Modelling firn thickness evolution during the last deglaciation: constraints on sensitivity to temperature and impurities, *Clim. Past*, 13, 833–853, <https://doi.org/10.5194/cp-13-833-2017>, 2017.
- Broadbent, S. R. and Hammersley, J. M.: Percolation processes: I. Crystals and mazes, *Math. Proc. Cambridge*, 53, 629–641, <https://doi.org/10.1017/S0305004100032680>, 1957.
- Eicher, O., Baumgartner, M., Schilt, A., Schmitt, J., Schwander, K., Stocker, T. F., and Fischer, H.: Climatic and insolation control on the high-resolution total air content in the NGRIP ice core, *Clim. Past*, 12, 1979–1993, <https://doi.org/10.5194/cp-12-1979-2016>, 2016.
- 15 Enting, I. G.: Statistics of firn closure: a simulation study, *J. Glaciol.*, 39, 133–142, <http://www.ingentaconnect.com/content/igsoc/jog/1993/00000039/00000131/art00014>, 1993.
- Fabre, A., Barnola, J.-M., Arnaud, L., and Chappellaz, J.: Determination of gas diffusivity in polar firn: comparison between experimental measurements and inverse modeling, *Geophys. Res. Lett.*, 27, 557–560, 2000.
- 20 Freitag, J., Kipfstuhl, S., and Laepple, T.: Core-scale radioscopic imaging: a new method reveals density–calcium link in Antarctic firn, *J. Glaciol.*, 59, 1009–1014, <https://doi.org/10.3189/2013JoG13J028>, 2013.
- Goujon, C., Barnola, J.-M., and Ritz, C.: Modeling the densification of polar firn including heat diffusion: Application to close-off characteristics and gas isotopic fractionation for Antarctica and Greenland sites, *J. Geophys. Res.*, 108, 4792, <https://doi.org/10.1029/2002JD003319>, 2003.
- 25 Gregory, S. A., Albert, M. R., and Baker, I.: Impact of physical properties and accumulation rate on pore close-off in layered firn, *Cryosphere*, 8, 91–105, <https://doi.org/10.5194/tc-8-91-2014>, 2014.
- Herron, M. M. and Langway, C. C.: Firn Densification: An Empirical Model, *J. Glaciol.*, 25, 373–385, <https://doi.org/10.3198/1980JoG25-93-373-385>, 1980.
- Johnsen, S. J., Clausen, H. B., Dansgaard, W., Gundestrup, N. S., Hansson, M., Jonsson, P., Steffensen, J. P., and Sveinbjornsdottir, A. E.: A "deep" ice core from East Greenland, *Medd. Grønland, Geoscience* 29, 1–22, 1992.
- 30 Jouzel, J., Lorius, C., Petit, J. R., Genthon, C., Barkov, N. I., Kotlyakov, V. M., and Petrov, V. M.: Vostok ice core: a continuous isotope temperature record over the last climatic cycle (160,000 years), *Nature*, 329, 403–408, <https://doi.org/10.1038/329403a0>, 1987.
- Jouzel, J., Masson-Delmotte, V., Cattani, O., Dreyfus, G., Falourd, S., Hoffmann, G., Minster, B., Nouet, J., Barnola, J.-M., Chappellaz, J., Fischer, H., Gallet, J. C., Johnsen, S., Leuenberger, M., Loulergue, L., Luethi, D., Oerter, H., Parrenin, F., Raisbeck, G., Raynaud, D., Schilt, A., Schwander, J., Selmo, E., Souchez, R., Spahni, R., Stauffer, B., Steffensen, J. P., Stenni, B., Stocker, T. F., Tison, J. L., Werner, M., and Wolff, E. W.: Orbital and Millennial Antarctic Climate Variability over the Past 800,000 Years, *Science*, 317, 793–796, <https://doi.org/10.1126/science.1141038>, 2007.



- Koehler, S. A., Hilgenfeldt, S., and Stone, H. A.: Liquid Flow through Aqueous Foams: The Node-Dominated Foam Drainage Equation, *Phys. Rev. Lett.*, 82, 4232–4235, <https://doi.org/10.1103/PhysRevLett.82.4232>, 1999.
- Legrand, M. and Mayewski, P.: Glaciochemistry of polar ice cores: A review, *Rev. Geophys.*, 35, 219–243, <https://doi.org/10.1029/96RG03527>, 1997.
- 5 Loulergue, L., Schilt, A., Spahni, R., Masson-Delmotte, V., Blunier, T., Lemieux, B., Barnola, J.-M., Raynaud, D., Stocker, T. F., and Chappellaz, J.: Orbital and millennial-scale features of atmospheric CH<sub>4</sub> over the past 800,000 years, *Nature*, 453, 383–386, <https://doi.org/10.1038/nature06950>, 2008.
- Martinerie, P., Lipenkov, V. Y., and Raynaud, D.: Correction of air-content measurements in polar ice for the effect of cut bubbles at the surface of the sample, *J. Glaciol.*, 36, 299–303, <http://www.ingentaconnect.com/content/igsoc/jog/1990/00000036/00000124/art00006>,  
10 1990.
- Martinerie, P., Raynaud, D., Etheridge, D. M., Barnola, J.-M., and Mazaudier, D.: Physical and climatic parameters which influence the air content in polar ice, *Earth Planet. Sc. Lett.*, 112, 1–13, <http://www.sciencedirect.com/science/article/pii/0012821X9290002D>, 1992.
- Mitchell, L. E., Buizert, C., Brook, E. J., Breton, D. J., Fegyveresi, J., Baggenstos, D., Orsi, A., Severinghaus, J., Alley, R. B., Albert, M., Rhodes, R. H., McConnell, J. R., Sigl, M., Maselli, O., Gregory, S., and Ahn, J.: Observing and modeling the influence of layering on  
15 bubble trapping in polar firn, *J. Geophys. Res.*, 120, 2558–2574, <https://doi.org/10.1002/2014JD022766>, 2015.
- Nguyen, T., Tran, T., Willemsz, T., Frijlink, H., Ervasti, T., Ketolainen, J., and Maarschalk, K.: A density based segmentation method to determine the coordination number of a particulate system, *Chem. Eng. Sci.*, 66, 6385–6392, <https://doi.org/10.1016/j.ces.2011.08.044>, 2011.
- Parrenin, F.: New modeling of the Vostok ice flow line and implication for the glaciological chronology of the Vostok ice core, *J. Geophys. Res.*, 109, <https://doi.org/10.1029/2004JD004561>, 2004.  
20
- Parrenin, F., Barker, S., Blunier, T., Chappellaz, J., Jouzel, J., Landais, A., Masson-Delmotte, V., Schwander, J., and Veres, D.: On the gas-ice depth difference ( $\Delta$  depth) along the EPICA Dome C ice core, *Clim. Past*, 8, 1239–1255, <https://doi.org/10.5194/cp-8-1239-2012>, 2012.
- Raynaud, D. and Lebel, B.: Total gas content and surface elevation of polar ice sheets, *Nature*, 281, 289–291, <https://doi.org/10.1038/281289a0>, 1979.
- 25 Raynaud, D., Lipenkov, V., Lemieux-Dudon, B., Duval, P., Loutre, M.-F., and Lhomme, N.: The local insolation signature of air content in Antarctic ice. A new step toward an absolute dating of ice records, *Earth Planet. Sc. Lett.*, 261, 337–349, <https://doi.org/10.1016/j.epsl.2007.06.025>, 2007.
- Schneebeli, M. and Sokratov, S. A.: Tomography of temperature gradient metamorphism of snow and associated changes in heat conductivity, *Hydrol. Process.*, 18, 3655–3665, <https://doi.org/10.1002/hyp.5800>, 2004.
- 30 Schwander, J.: The transformation of snow to ice and the occlusion of gases, in: *The Environmental Record in Glaciers and Ice Sheets*, edited by Oeschger, H. and Langway, C. C., pp. 53–67, John Wiley & Sons, Chichester, 1989.
- Schwander, J. and Stauffer, B.: Age difference between polar ice and the air trapped in its bubbles, *Nature*, 311, 45–47, <https://doi.org/10.1038/311045a0>, 1984.
- Schwander, J., Barnola, J.-M., Andrié, C., Leuenberger, M., Ludin, A., Raynaud, D., and Stauffer, B.: The age of the air in the firn and the  
35 ice at Summit, Greenland, *J. Geophys. Res.*, 98, 2831–2838, <https://doi.org/10.1029/92JD02383>, 1993.
- Severinghaus, J. and Battle, M.: Fractionation of gases in polar ice during bubble close-off: New constraints from firn air Ne, Kr and Xe observations, *Earth Planet. Sc. Lett.*, 244, 474–500, <https://doi.org/10.1016/j.epsl.2006.01.032>, 2006.





- Severinghaus, J. P., Sowers, T., Brook, E. J., Alley, R. B., and Bender, M. L.: Timing of abrupt climate change at the end of the Younger Dryas interval from thermally fractionated gases in polar ice, *Nature*, 391, 141–146, 1998.
- Sowers, T., Bender, M., Raynaud, D., and Korotkevich, Y. S.:  $\delta^{15}\text{N}$  of  $\text{N}_2$  in air trapped in polar ice: A tracer of gas transport in the firn and a possible constraint on ice age-gas age differences, *J. Geophys. Res.*, 97, 15 683, <https://doi.org/10.1029/92JD01297>, 1992.
- 5 Stauffer, B., Schwander, J., and Oeschger, H.: Enclosure of air during metamorphosis of dry firn to ice, *Ann. Glaciol.*, 6, 108–112, <http://www.ingentaconnect.com/content/igsoc/agl/1985/00000006/00000001/art00025>, 1985.
- Trudinger, C. M., Enting, I. G., Etheridge, D. M., Francey, R. J., Levchenko, V. A., Steele, L. P., Raynaud, D., and Arnaud, L.: Modeling air movement and bubble trapping in firn, *J. Geophys. Res.*, 102, 6747–6763, <https://doi.org/10.1029/96JD03382>, 1997.
- van der Marck, S. C.: Percolation thresholds of the duals of the face-centered-cubic, hexagonal-close-packed, and diamond lattices, *Phys. Rev. E*, 55, 6593–6597, <https://doi.org/10.1103/PhysRevE.55.6593>, 1997.
- 10 Vinther, B. M., Buchardt, S. L., Clausen, H. B., Dahl-Jensen, D., Johnsen, S. J., Fisher, D. A., Koerner, R. M., Raynaud, D., Lipenkov, V., Andersen, K. K., Blunier, T., Rasmussen, S. O., Steffensen, J. P., and Svensson, A. M.: Holocene thinning of the Greenland ice sheet, *Nature*, 461, 385–388, <https://doi.org/10.1038/nature08355>, 2009.
- Weiler, K.: On the composition of firn air and its dependence on seasonally varying atmospheric boundary conditions and the firn structure, Ph.D. thesis, University of Bern, 2008.
- 15 Wierman, J. C. and Naor, D. P.: Desirable properties of universal formulas for percolation thresholds, *Congressus Numerantium*, pp. 125–142, 2003.



**Table 1.** Details on the analyzed cores. Mean annual temperature is denoted by  $\bar{T}$  and an estimate of yearly accumulation by  $\dot{a}$ .

Drill site	Year	Elevation [m]	$\bar{T}$ [ $^{\circ}\text{C}$ ]	$\dot{a}$ [ $\text{kg m}^{-2} \text{a}^{-1}$ ]	Depth interval [m]	No. of data points
RECAP_S2 (Renland, Greenland) <sup>†</sup>	2015	2296	-18	460	49–73	246
B49 (Kohnen station, East Antarctica)*	2012/13	2881	-44	65	73–90	303
B53 (Dome Fuji, East Antarctica)*	2012/13	3726	-55	30	76–106	614

<sup>†</sup> Johnsen et al. (1992)

\* Unpublished data, the accumulation rates are based on a preliminary volcanic layer dating.

**Table 2.** Results of least squares fitting our parametrisation to the obtained data.

Data set	$\Phi_{crit}$	$\lambda_1$	$\lambda_2$	$b$	$R^2$
RECAP_S2	0.1005	62.45	47.34	0.4816	0.9744
B49	0.0985	169.57	51.55	0.5797	0.9801
B53	0.1000	206.36	48.06	0.7072	0.9603

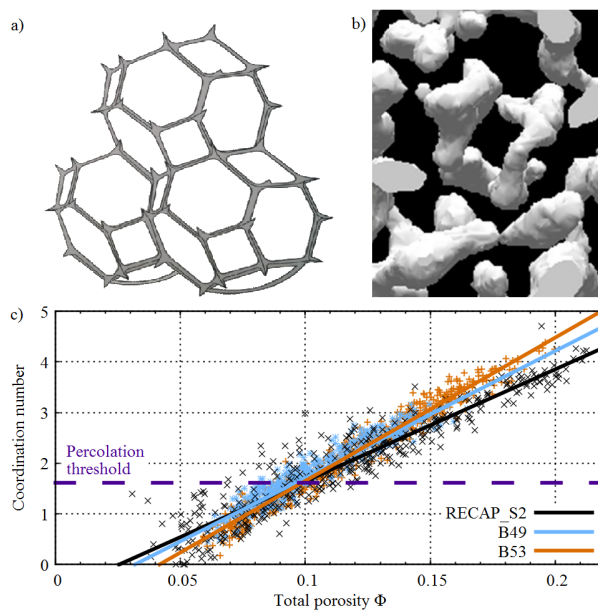


**Figure 1.** a) A structure consisting of three packed tetrakaidecahedra. The white bodies do represent ice crystals, the gray edges the pore network. b) Example of a 3D scan, the pore network is shown in white. c) Coordination number versus total porosity for our measurements. The threshold for close-off predicted by percolation theory has been marked.

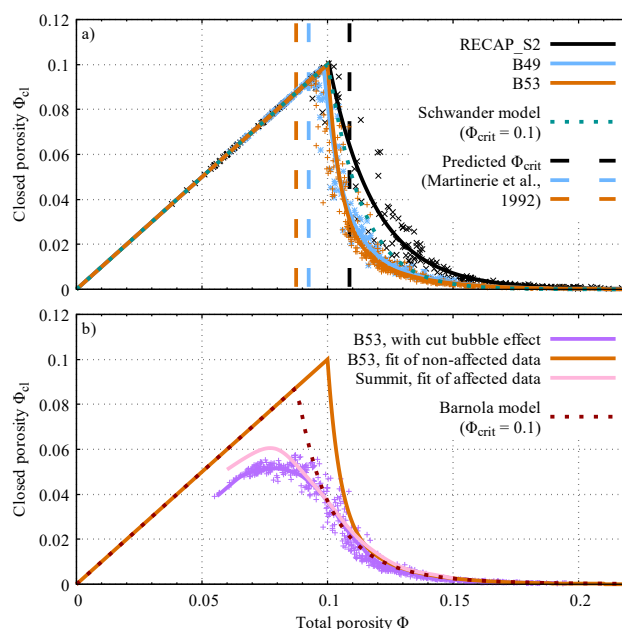


**Figure 2.** Closed versus total porosity for a) the analyzed cores in comparison with commonly expected values and b) B53 ignoring cut bubbles compared to previous results from Summit, Greenland (Schwander et al., 1993). The solid lines indicate least squares fits for the respective core, the short-dashed lines represent model results (Schwander, 1989; Goujon et al., 2003) for the given parameters and the long-dashed lines mark the critical porosity values predicted by the previously observed temperature dependence (Martinerie et al., 1992).

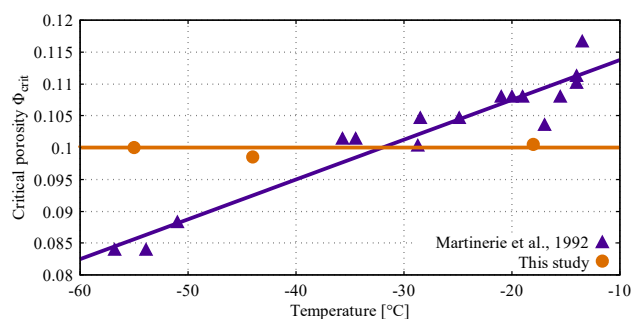


**Figure 3.** Critical porosity versus temperature. The given linear relation is commonly fit to the data of Martinerie et al. (1992). Their study was based on 495 data points for sixteen cores (with a minimum of only two measurements for one core). We analyzed 1163 samples for three cores (see Table 1).